DOI: 10.1002/chem.200700961

Photoinduced Fe–Cp Bond Cleavage and Insertion Reactions of Strained Silicon- and Sulphur-Bridged [1]Ferrocenophanes in the Presence of Transition-Metal Carbonyls

Nga Sze Ieong,[a] Wing Yan Chan,[b] Alan J. Lough,[b] Mairi F. Haddow,[a] and Ian Manners*[a, b]

Abstract: The photochemical reactions of the moderately strained sila[1]ferrocenophane [Fe(η-C_5H_4)$_2$$SiPh_2$] (**1**) and the highly strained thia[1]ferrocenophane [Fe(η-C_5H_4)$_2$S] (**8**) with transition-metal carbonyls ([$Fe(CO)_5$], [$Fe_2(CO)_9$] and [$Co_2(CO)_8$]) have been studied. The use of metal carbonyls has allowed the products of photochemically induced Fe-cyclopentadienyl (Cp) bond cleavage reactions in the [1]ferrocenophanes to be trapped as stable, characterisable products. During the course of these studies the synthesis of **8** from [Fe(η-$C_5H_4Li)_2$·TMEDA] (TMEDA = *N*,*N*,*N*′,*N*′-tetramethylethylenediamine) and $S(SO_2Ph)_2$ has been significantly improved by a change of reaction solvent and temperature. Photochemical reaction of **1** with excess [$Fe(CO)_5$] in THF gave the dinuclear complex [$Fe_2(CO)_2$(μ-CO)$_2$(η-C_5H_4)$_2$$SiPh_2$] (**9**). The analogous photolytic reaction of **8** with [$Fe(CO)_5$] in THF gave cyclic dimer [Fe(η-C_5H_4)$_2$S]$_2$ (**10**) and [$Fe_2(CO)_2$(μ-CO)$_2$(η-C_5H_4)$_2$S] (**11**), with the former being the major product. Photolysis of **1** with [$Co_2(CO)_8$] afforded the remarkable tetrametallic dimer [$(CO)_2$Co(η-C_5H_4)$SiPh_2$(η-C_5H_4)Fe$(CO)_2$]$_2$ (**13**). The corresponding photochemical reaction of **8** with [$Co_2(CO)_8$] gave a trimetallic insertion product in high conversion, [$Co(CO)_4(CO)_2$Fe(η-C_5H_4)S(η-C_5H_4)Co$(CO)_2$] (**14**). These reactivity studies show that UV light promotes Fe–Cp bond cleavage reactions of both of the [1]ferrocenophanes **1** and **8**. We have found that, whereas the less strained sila[1]ferrocenophane **1** requires photoactivation for Fe–Cp bond insertions to occur, the highly strained thia[1]ferrocenophane **8** undergoes both irradiative and non-irradiative insertions, although the latter occur at a slower rate. Our results suggest that such photoinduced bond cleavage reactions may be general and applicable to other related strained organometallic rings with π-hydrocarbon ligands.

Keywords: cyclopentadienyl ligands · ferrocenophanes · insertion · metallocenes · photolysis

Introduction

Although studies of the synthesis and reactivity of strained cyclic organic compounds are very extensive, analogous strained metal-containing rings are much less explored. Since the discovery of the first example, sila[1]ferrocenophane **1** in 1975 by Osborne and co-workers,[1] strained [1]ferrocenophanes **2** have attracted considerable attention and have inspired growing interest in a range of related species containing various metals,[2–11] bridging elements[12–25] and even π-hydrocarbon ligands.[26–35] The angle created by the planes of the two Cp rings in a ferrocenophane, generally denoted as α, serves as a convenient qualitative measure of the degree of strain present.[36] One of the most important factors that govern α, and hence the reactivity of [1]ferrocenophanes, is the identity of the bridging atom E. Upon reduction of the covalent radius of the bridging element, [1]ferrocenophanes exhibit increased strain, with larger tilt-angles and an increased bathochromic shift and intensity for the longest wavelength electronic transition.[37] These results have been explained in terms of a decreased HOMO–LUMO gap and increased ligand character for the LUMO on increasing α.[20,37] The inherent ring-strain in ferrocenophanes also renders these species highly susceptible to ring-

[a] N. S. Ieong, M. F. Haddow, Prof. I. Manners
School of Chemistry
University of Bristol
Cantock's Close, Bristol, BS8 1TS (UK)
Fax: (+44) 117–929–0509
E-mail: Ian.Manners@bristol.ac.uk

[b] W. Y. Chan, Dr. A. J. Lough, Prof. I. Manners
Department of Chemistry
University of Toronto
80 St. George Street, Toronto, Ontario, M5S 3H6 (Canada)

opening reactions. For example, sila[1]ferrocenophanes such as **2** ($ER_x = SiMe_2$) ring-open upon treatment with a protic source, such as HCl and MeOH, which results in the cleavage of the *ipso*-Cp-C–Si bond to yield **3** (X = Cl[38] or OH[17] respectively). Sila[1]ferrocenophanes also undergo thermal,[39,40] anionic[41] or transition-metal-catalysed[42,43] ring-opening polymerisations (ROP), to give polyferrocenylsilanes through cleavage of the *ipso*-Cp-C–Si bond. When reacted with Pt(0) complexes, sila[1]ferrocenophanes yield platinasila[2]ferrocenophanes such as **4** by insertion of a Pt fragment into the Si–Cp bond.[44]

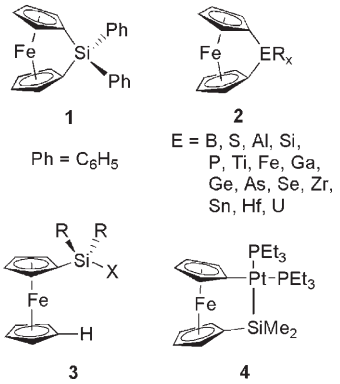

Although extensive previous studies have shown that [1]ferrocenophanes predominantly undergo ring-opening chemistry at the bridging atom E–Cp bond, recent reports have highlighted that reactivity at the Fe–Cp bond can also occur, especially on photoactivation. For example, highly tilted bora[1]ferrocenophane **5** ($\alpha = 32°$), has been shown to stoichiometrically react with $[Fe(CO)_5]$ (or $[Fe_2(CO)_9]$) and $[Co_2(CO)_8]$ under photoirradiation to afford products **6** and **7**, respectively, through insertion of metal carbonyl fragments into the Fe–Cp bond.[12] Miyoshi and co-workers have demonstrated that strained phospha[1]ferrocenophanes ($\alpha \approx 27°$) undergo unprecedented Fe–Cp bond cleavage upon photoirradiation and, in the presence of donor solvents such as THF, photolytic ROP was detected.[45,46] By using $[C_5H_5]^-$ ions as the initiator we have recently shown that photocontrolled living polymerisations of sila[1]ferrocenophanes can be achieved via Fe–Cp bond cleavage.[47,48] In addition, in the presence of phosphorus-donor ligands sila[1]ferrocenophanes have been shown to undergo reversible haptotropic shifts of the Cp ligand from η^5 to η^1 on phosphine coordination.[49] The subtle dependence of the reactivity of [1]ferrocenophanes on the nature of the bridging atom is demonstrated by the following example: whereas the aforementioned treatment of bora[1]ferrocenophanes **5** with metal carbonyls leads to reactivity at the Fe–Cp bond to yield **6** and **7**,[12] the analogous reaction using tin-bridged[1]ferrocenophanes yields products arising from the insertion of metal carbonyl fragments into the Sn–Cp bond.[50]

To provide further insight into the contrasting reactivity of [1]ferrocenophanes with different bridging atoms, we report comparative studies of the photolytic reactivity of sila[1]ferrocenophane **1** ($\alpha = 19.2°$) and the more highly strained thia[1]ferrocenophane **8** ($\alpha = 31.1°$) with metal carbonyls. In our attempts to characterise the various modes of potential reactivity, metal carbonyl complexes were viewed as ideal coreactants as the bonding flexibility of CO is likely to maximise the possibility of stable product isolation.

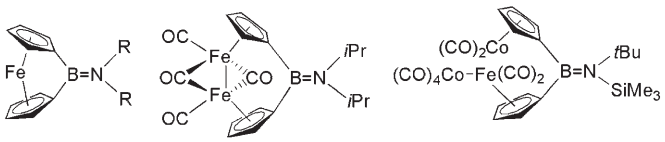

Results and Discussion

Synthesis of sila[1]ferrocenophane 1 and thia[1]ferrocenophane 8: Sila[1]ferrocenophane **1** was prepared by the previously published method and involved the reaction of dilithioferrocene $[Fe(\eta\text{-}C_5H_4Li)_2 \cdot TMEDA]$ (TMEDA = *N*,*N*,*N*′,*N*′-tetramethylethylenediamine) with dichlorodiphenylsilane Ph_2SiCl_2.

The highly strained species **8** has been previously prepared in low yield (≈30%) by the reaction of $[Fe(\eta\text{-}C_5H_4Li)_2 \cdot TMEDA]$ with the trisulphide $S(SO_2Ph)_2$ on combination with THF at −196 °C and subsequent warming to room temperature. However, there were some major problems with this method for us to overcome.[20] Firstly, it was a potentially dangerous preparation as an explosion can occur once the reaction starts. Secondly, the THF soluble byproduct $Li[SO_2Ph]$ decomposes **8** by inducing ring-opening oligomerisation at low temperatures (≈ −40 °C). We have improved the synthesis by a change of the reaction medium from pure THF to a 3:2 mixture of THF and hexane and thereby increasing the reaction temperature from −196 °C to −78 °C (Scheme 1). The modified synthesis gave purple crystalline **8**, which was analytically pure (by ^1H NMR spectroscopy) in 30% yield (Scheme 1).

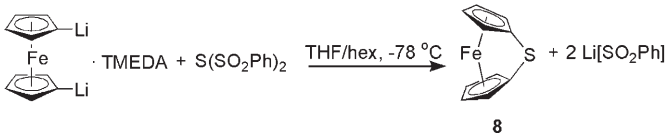

Scheme 1. Synthesis of **8**.

Photolytic reactivity of [1]ferrocenophanes 1 and 8 with $[Fe(CO)_5]$ and $[Fe_2(CO)_9]$

*Photolytic reaction of **1** with $[Fe(CO)_5]$, characterisation of **9***: Reaction of **1** with excess $[Fe(CO)_5]$ under UV irradiation ($\lambda > 310$ nm) in a weakly coordinating solvent (THF) gave the new product **9**, formed from the insertion of a $[Fe(CO)_4]$ fragment into a Fe–Cp bond, in ≈95% yield by ^1H NMR spectroscopy (5% of unreacted **1** was detected) (Scheme 2).

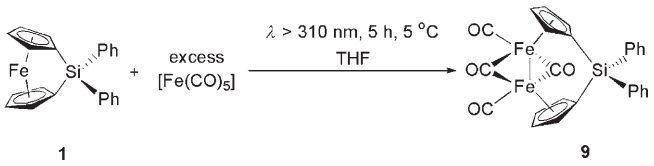

1 9

Scheme 2. Photolytic reaction of **1** with $[Fe(CO)_5]$.

The Cp protons of **9** appeared as two sets of pseudo-triplets, which exhibit downfield shifts ($\delta = 4.94$, 5.12 ppm) relative to those of the starting material **1** ($\delta = 4.10$, 4.40 ppm). Shifts of such magnitude have been previously observed for analogous species (e.g., **6**[12] and $[Fe_2(CO)_2(\eta\text{-}CO)_2(\eta^5\text{-}C_5H_4)_2(SiMe_2)]$.[51] The mass spectrum of **9** showed the presence of the molecular ion ($m/z = 534$) and the successive loss of four carbonyls, which strongly suggests the insertion of the $[Fe(CO)_4]$ fragment to form **9**. Moreover, the elemental analysis also supported the proposed structure **9**.

Control reactions were also performed. First, photolysis of **1** alone in THF gave no detectable reaction after 5 h. Moreover, in the dark, treatment of **1** with $[Fe_2(CO)_9]$ in THF led only to the recovery of unreacted **1** after prolonged stirring for 12 h. These studies indicated that the photoactivation of **1** is necessary for reactions with iron carbonyls to be detected (Scheme 2).

*Photolytic reaction of **8** with $[Fe(CO)_5]$*: In contrast to **1**, the photochemical reaction of **8** with a slight excess of $[Fe(CO)_5]$ in THF at 5 °C afforded two products, the orange crystalline cyclic dimer **10** and the light brown crystalline Fe–Cp bond insertion product **11**. These species were separated by solvent extraction as shown in Scheme 3. The products were identified by NMR and IR (for **11**) spectroscopy, mass spectrometry, elemental analysis (for **10**) and X-ray crystallography (Scheme 3).

*Isolation and characterisation of the cyclic dimer **10***: The photochemical reaction of **8** with $[Fe(CO)_5]$ in THF (Scheme 3) gave **10** as the dominant product. Upon extraction with toluene and then removal of solvent, **10** was isolated as an air-stable yellow powder in 38% yield. A higher yield of **10** was obtained by photolysing **8** alone in THF for 3 h at 5 °C (Scheme 4a, isolated yield ≈54%), with concomitant formation of other oligomers of **8** as byproducts. The latter can be easily removed due to their insolubility in common organic solvents.[20]

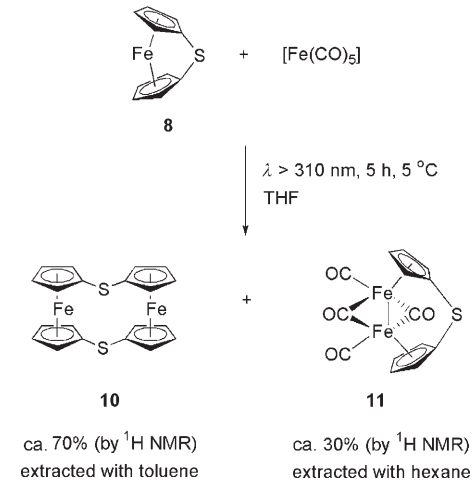

Scheme 3. Photolytic reaction of **8** with $[Fe(CO)_5]$.

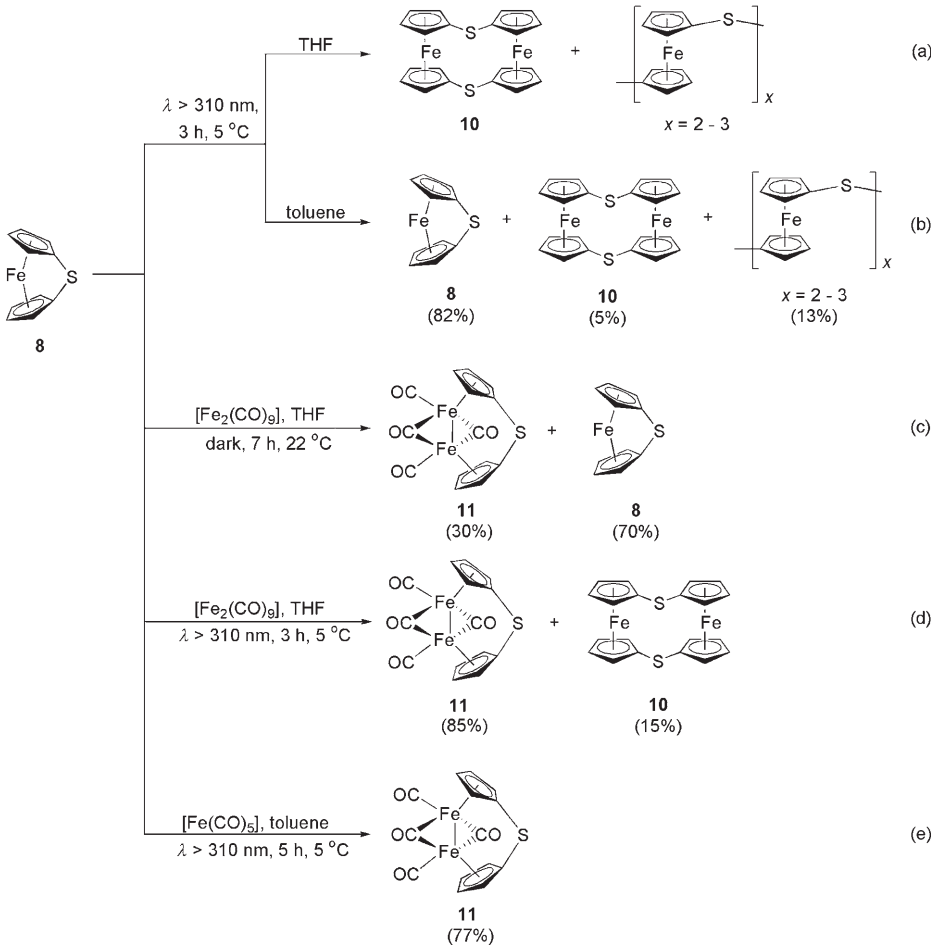

Scheme 4. Reactivity studies of **8** with iron carbonyls.

The cyclic dimer **10** can readily be distinguished from the $[Fe(CO)_4]$ insertion product **11** by ^{1}H NMR spectroscopy. The Cp protons of both **10** and **11** are observed as pairs of pseudo-triplets with those of the former shifted slightly upfield ($\delta = 3.90$, 4.56 ppm) while those of the latter are more downfield ($\delta = 4.43$, 4.73 ppm) relative to the starting material **8** ($\delta = 3.96$, 4.61 ppm).[20]

Since the X-ray crystal structure of the first [1.1]ferrocenophane was reported by Watts et al. in 1967,[52] such species have attracted significant attention, owing to their unusual structural and redox properties.[53] Analogous [1.1]ferrocenophanes bearing ER_x bridging groups, in which E ranges from Group 13 (B,[54] Al, Ga, In[55]), Group 14 (C[56] Si,[53,57] Sn[19]) to Group 15 (P[58,59]), have also been published and their properties extensively studied. Nonetheless, to the best of our knowledge, compound **10** is the first example of a Group-16-bridged [1.1]ferrocenophane. The ^{1}H NMR spectrum of **10** showed resonances (see above) in the typical Cp regions for [1.1]ferrocenophanes.[54,59] It has been previously noted that, in general, the greater the ring-strain in [1]ferrocenophanes, the more upfield shifted the *ipso*-Cp-C ^{13}C resonance. The fact that the *ipso*-^{13}C NMR signal of **10** is considerably downfield shifted ($\delta = 87.3$ ppm) relative to that of **8** ($\delta = 14.3$ ppm), suggests that ring-strain has been significantly relieved upon dimerisation. Recrystallisation from toluene at $-40\,^\circ$C gave orange crystals of the cyclic dimer **10** suitable for single-crystal X-ray diffraction study. The molecular structure and selected bond lengths and bond angles of **10** are shown in Figure 1.

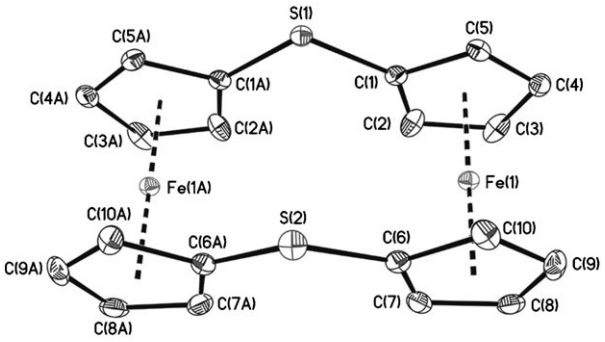

Figure 1. Molecular structure of **10** (thermal ellipsoids at 30% probability, hydrogen atoms have been omitted for clarity). Selected bond lengths [Å] and bond angles [°]: S(1)–C(1A) 1.752(3), S(1)–C(1) 1.752(3), S(2)–C(6A) 1.758(3), S(2)–C(6) 1.758(3), C(1A)-S(1)-C(1) 108.6(2), C(6A)-S(2)-C(6) 111.1(2).

It has been reported that an ER_2-bridged [1.1]ferrocenophane can adopt a *syn* and/or *anti*-conformation depending on the balance between two types of intramolecular steric repulsions.[60] For **10**, both isomers might be expected. However, the distinct set of pseudo-triplets for the Cp protons in the ^{1}H NMR spectrum suggests the presence of only one isomer in solution at 22 °C. Moreover, the method of recrystallisation employed yielded presumably only the *syn* isomer. Nevertheless, the existence of the *anti* isomer in solution is not to be ruled out.

Figure 1 shows the molecular structure of **10**. The Cp rings of **10** adopt essentially eclipsed conformations as is typical for *syn*-[1.1]ferrocenophanes.[58] The very small ring-tilt ($\alpha = 1.76^\circ$) for each of the ferrocenyl units indicates that the Cp rings are almost parallel. In contrast to the highly strained starting material **8** (C(1)-S-C(6) = 89.03(9)°), the bridge angle of **10** (C(1A)-S(1)-C(1) = 108.6(2)°, C(6A)-S(2)-C(6) = 111.1(2)°) shows that each of the sulphur atoms adopts an almost ideal tetrahedral angle.

*Characterisation of **11***: From our initial attempts to isolate **11**, we found that the use of the donor solvent THF results in the formation of cyclic dimer **10** as the major product in the photochemical reaction of **8** with $[Fe(CO)_5]$ (Scheme 3). In contrast, upon changing the reaction solvent to relatively non-polar toluene, **11** was isolated in high yield virtually free of **10** (Scheme 4e). The formation of **11** in substantially lower yield was achieved by the reaction of **8** with $[Fe_2(CO)_9]$ in THF (which generates $[Fe(CO)_4THF]$ directly) in the absence of light (Scheme 4c). The ^{1}H NMR spectrum of **11** showed two distinct pseudo-triplets for Cp protons at $\delta = 4.43$ and 4.73 ppm, significantly shifted downfield from those of **8** ($\delta = 3.96$, 4.61 ppm). Similarly, the $^{13}C\{^1H\}$ NMR spectrum of **11** showed two resonances for Cp carbons at $\delta = 83.5$ and 99.7 ppm, both of which are considerably shifted downfield relative to **8** ($\delta = 76.9$ and 82.1 ppm). Downfield shifts of such magnitudes are typical for [1]ferrocenophanes after insertion of a $[Fe(CO)_4]$ moiety between the Cp rings.[12] The IR spectrum of **11** showed peaks attributed to terminal ($\tilde{\nu} = 1978\ cm^{-1}$) and bridging ($\tilde{\nu} = 1806\ cm^{-1}$) carbonyl ligands. These peak positions are similar to those of the boron-bridged analogue **6** ($\tilde{\nu} =$ 1990 cm^{-1} (CO), 1781 cm^{-1} (μ-CO)).[12] The mass spectrum of **11** showed the molecular ion at $m/z = 384$ and the subsequent loss of four carbonyl ligands, which suggests that insertion of the $[Fe(CO)_4]$ fragment into a Fe–Cp bond of **8** gave **11**.

To confirm the assigned structure and compare structural details, a single-crystal X-ray diffraction study was performed for **11**. Figure 2 shows the molecular structure of **11** and Table 1 lists selected bond lengths and bond angles. Compound **11** is the sulphur-bridged analogue of **6**, which was formed from an analogous reaction using a bora[1]ferrocenophane.[12] Compound **11** is presumably formed by insertion of a photochemically generated $[Fe(CO)_4]$ fragment into the Fe–Cp bond, followed by rearrangement of the carbonyl ligands. The insertion of the $[Fe(CO)_4]$ moiety between the Cp rings dramatically increases the C(1A)-S(1)-C(1) angle in **11** (100.76(17)°) from the corresponding angle in **8** (89.03(9)°)[61] Compared to analogous structures, *cis*-$[(\eta^5\text{-Cp})Fe(CO)_2]_2$ (d(Fe–Fe) = 2.533 Å)[62] and $[Fe_2(CO)_2(\eta\text{-}CO)_2(\eta^5\text{-}C_5H_4)_2SiMe_2]$ (d(Fe–Fe) = 2.513(3) Å),[51] the Fe–Fe bond distance of **11** (2.4912(7) Å) is significantly shorter, owing to the introduction of the small bridging S atom.

From the photolytic reactivity studies with **8**, we postulate the mechanism shown in Scheme 5. Photochemical reaction of **8** and $[Fe(CO)_5]$ in THF is proposed to proceed by two

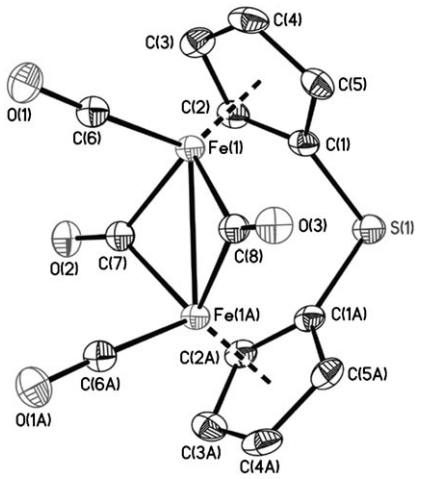

Figure 2. Molecular structure of **11** (thermal ellipsoids at 30% probability, hydrogen atoms have been omitted for clarity).

Table 1. Selected bond lengths [Å] and bond angles [°] for **11**.

Fe(1)−C(6)	1.762(3)	C(6)-Fe(1)-C(7)	90.19(13)
Fe(1)−C(7)	1.921(3)	C(6)-Fe(1)-C(8)	90.65(13)
Fe(1)−C(8)	1.926(3)	C(7)-Fe(1)-C(8)	95.62(11)
Fe(1)−C(4)	2.097(3)	C(6)-Fe(1)-Fe(1A)	105.99(9)
Fe(1)−C(1)	2.109(3)	C(7)-Fe(1)-Fe(1A)	49.57(8)
Fe(1)−C(3)	2.111(3)	C(8)-Fe(1)-Fe(1A)	49.70(7)
Fe(1)−C(5)	2.117(3)	C(1A)-S(1)-C(1)	100.76(17)
Fe(1)−C(2)	2.137(3)	α	76.60(9)
Fe(1)−Fe(1A)	2.4912(7)		
S(1)−C(1A)	1.772(3)		
S(1)−C(1)	1.772(3)		
C(6)−O(1)	1.151(3)		
C(7)−O(2)	1.178(4)		
C(8)−O(3)	1.177(4)		
Fe(1A)−C(7)	1.921(3)		

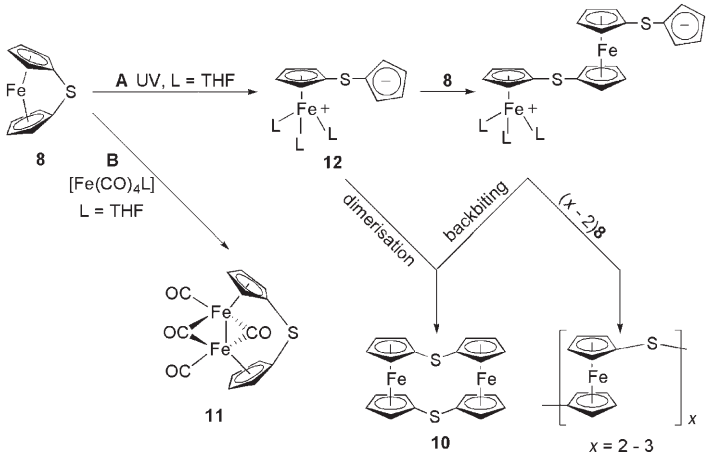

Scheme 5. Proposed mechanism for the formation of **10** and **11**.

competing pathways (Scheme 5, A and B). The approximate ratio of the products **10** and **11** in this solvent (70:30 by ^{1}H NMR spectroscopy) suggests that the major route involves the initial photoinduced cleavage of the Fe−Cp bond to form the zwitterionic species **12** (path A). A comparison of the reactions shown in Scheme 4a,b suggests that the formation of the cyclic dimer **10** in high yield requires both UV light to cleave the Fe−Cp bond and a donor solvent (THF) to stabilise the Fe centre. Conversely, it appears that in the absence of light and/or a coordinating solvent, the formation of **10** is inhibited and product **11** is preferred, as observed in Scheme 4c,e respectively. However, it should be noted that irradiative insertions occur significantly faster than their non-irradiated analogs. The formation of **11** appears to occur via a pathway involving direct insertion of $[Fe(CO)_4]$ fragments into the Fe−Cp bond of **8** (Scheme 5, path B) as the same product results from the treatment of the latter with $[Fe_2(CO)_9]$ in THF in the absence of light, which generates $[Fe(CO)_4(THF)]$ in situ (Scheme 4c). Interestingly, for the silicon-bridged [1]ferrocenophane **1**, the operation of the analog of pathway B in Scheme 5 requires photoactivation of the Fe−Cp bond. Moreover, the analogous pathway to A does not operate to a significant extent. This may be a consequence of the lower degree of ring-strain present in **1**.

In the absence of light, **8** reacted with $[Fe(CO)_4THF]$ (generated in situ from $[Fe_2(CO)_9]$) after 7 h at 22 °C to give **11** in 30% conversion by ^{1}H NMR spectroscopy (Scheme 4c). In key contrast, the analogous reaction in the presence of UV light occurred dramatically faster with 85% conversion to **11** after 3 h (Scheme 4d). The above studies show that even though **8** undergoes both non-irradiative and irradiative insertions, the rate of the latter is significantly faster. Combining these results and the parallel studies of **1**, we have illustrated that UV light promotes Fe−Cp bond cleavage in both species, with the more strained **8** demonstrating higher reactivity.

Photolytic reactivities of [1]ferrocenophanes 1 and 8 with dicobalt octacarbonyl: The studies thus far have shown that both the moderately strained sila[1]ferrocenophane **1** and the highly strained thia[1]ferrocenophane **8** react photochemically with $[Fe(CO)_5]$ and $[Fe_2(CO)_9]$ to give products from Fe−Cp bond cleavage and insertion reactions but with notable differences in behaviour. To provide further insight into these phenomena, we have also examined parallel reactions with $[Co_2(CO)_8]$.

*Photolytic reaction of **1** with $[Co_2(CO)_8]$, synthesis of **13***: After mixing equimolar quantities of **1** with $[Co_2(CO)_8]$ in THF, the resulting dark red solution was photolysed at 5 °C for 7 h (Scheme 6a). The solvent was then removed in vacuo giving a dark brown solid. The ^{1}H NMR spectrum of the residue showed that the reaction proceeded to 80% conversion of **1**. Recrystallisation from hexane at −40 °C afforded dark brown crystals of the remarkable product **13** in 36% yield.

The ^{1}H NMR spectrum of **13** showed two well-defined resonances for Cp protons (δ = 4.50, 4.73 ppm) which are significantly shifted downfield relative to those of **1** (δ = 4.10, 4.40 ppm). Moreover the ^{13}C{^{1}H} NMR spectrum showed four closely spaced peaks in the typical Cp region at (δ = 92.8, 91.9, 90.6, 89.8 ppm) which are also considerably shifted downfield compared to those in **1** (δ = 77.9,

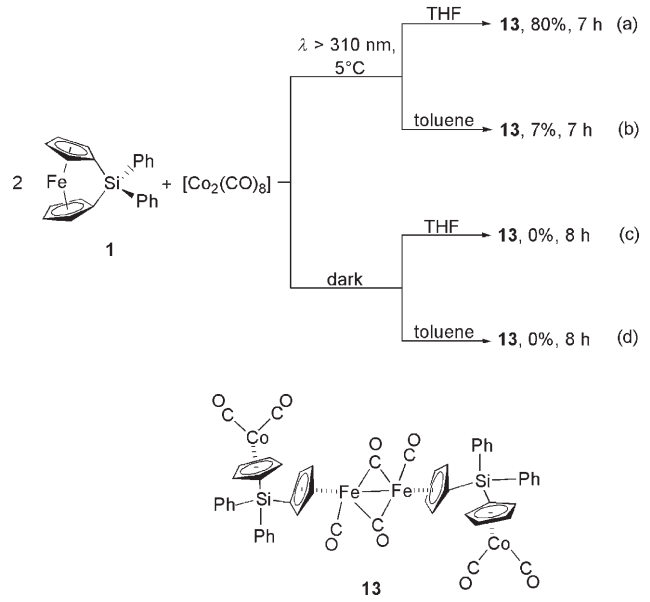

Scheme 6. Reactivity studies of **1** with $[Co_2(CO)_8]$.

76.7 ppm).[63] The fact that the number of $^{13}C\{^1H\}$ NMR resonances in the Cp region is twice that of **1** suggests that there are two types of Cp rings, each of which gives rise to two distinct peaks attributed to the α and β carbons.

To confirm the assigned structure, we performed a single-crystal X-ray diffraction study on **13**. Figure 3 shows the molecular structure of **13** and Table 2 lists selected bond lengths and bond angles.

The molecular structure confirmed that the compound is the novel tetrametallic insertion product **13**. The product contains two $[(\eta\text{-}C_5H_4)Co(CO)_2]$ fragments linked together by two molecules derived from ring-opened **1**, which are in turn connected by an Fe–Fe bond.

To gain further insight into the $[Co_2(CO)_8]$ reactions, various conditions were employed and the course of the trans-

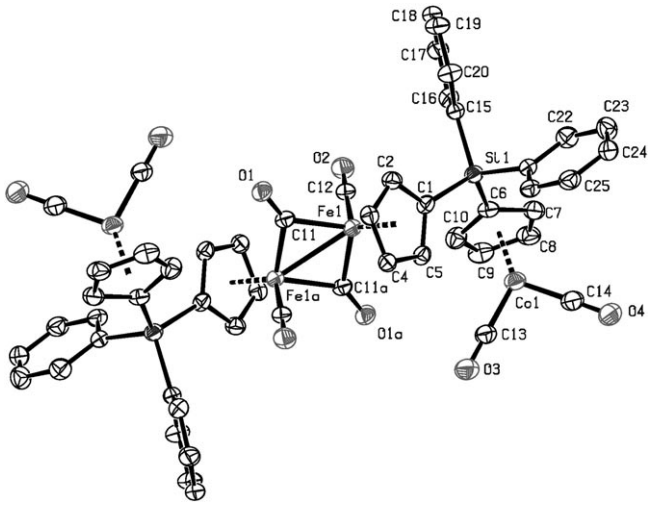

Figure 3. Molecular structure of **13** (thermal ellipsoids at 30% probability, hydrogen atoms have been omitted for clarity).

Table 2. Selected bond lengths [Å] and bond angles [°] for **13**.

Fe1–C12	1.745(6)	C11a-Fe1-C11	96.9(2)
Fe1–C11a	1.903(6)	C12-Fe1-Fe1a	95.5(2)
Fe1–C11	1.932(6)	C11a-Fe1-Fe1a	48.96(18)
Fe1–Fe1a	2.5422(18)	C13-Co1-C14	93.4(3)
Co1–C13	1.732(7)	Fe1a-C11-Fe1	83.1(2)
Co1–C14	1.742(8)		
C11–O1	1.179(6)		
C12–O2	1.164(6)		

formation monitored by ^1H NMR spectroscopy. A change from THF (Scheme 6a) to the relatively less coordinating solvent, toluene (Scheme 6b), dramatically reduced the conversion from 80% to 7%. Significantly, no reaction was detected between **1** and $[Co_2(CO)_8]$ in either THF (Scheme 6c) or toluene (Scheme 6d) in the absence of light. This indicates that photoactivation of **1** is necessary for Fe–Cp bond insertion reactions as found for the case of iron carbonyls.

The detailed mechanism of the formation of **13** is not obvious, but clearly the photochemical reaction of **1** with $[Co_2(CO)_8]$ leads to cleavage of the Fe–Cp bond and an insertion of a $[Co(CO)_4]$ fragment. A plausible mechanism involves dimerisation of the initial insertion product (which may also be photochemically promoted) followed by carbonyl rearrangements to give a structure free of heteronuclear metal–metal bonds (Scheme 7).

Compound **13** is an unusual analogue of the well-known dimer *trans*-$[(\eta^5\text{-}C_5H_4)Fe(CO)_2]_2$.[62] The major structural difference is that both the Fe coordinated Cp rings in **13** are connected to the silicon atoms of the $[SiPh_2(\eta^5\text{-}C_5H_4)Co(CO)_2]$ fragments, which are trans to one another. Notably, the Fe–Fe distance in **13** (2.542(3) Å) is comparable to that in $[(\eta^5\text{-}C_5H_4)Fe(CO)_2]_2$ (2.533 Å).[62]

*Photolytic reaction of **8** with $[Co_2(CO)_8]$, synthesis of **14***: The equimolar reaction of sulphur-bridged [1]ferrocenophane **8** with $[Co_2(CO)_8]$ under UV irradiation in THF for 1 h at 5 °C gave a dark maroon oil with 100% conversion as determined by ^1H NMR spectroscopy (Scheme 8a). Despite numerous attempts, the oily product could not be purified beyond ≈95% (by ^1H NMR spectroscopy) and no X-ray quality crystals could be obtained. In addition, the product was labile at room temperature and slowly transformed into other uncharacterised products on storage. Nevertheless, convincing existence of the proposed structure for the product **14** was provided by the use of a variety of spectroscopic analyses.

The ^1H NMR spectrum of **14** showed four distinct signals for Cp protons at $\delta = 3.99$, 4.11, 4.34 and 4.62 ppm, which are shifted slightly downfield relative to those of **8** ($\delta = 3.96$, 4.61 ppm). Moreover, the corresponding $^{13}C\{^1H\}$ NMR spectrum showed four closely spaced peaks for the Cp carbons at $\delta = 84.7$, 86.2, 86.3 and 89.1 ppm, which are also shifted downfield compared to those in **8** ($\delta = 76.9$ and 82.1 ppm).[20] The increase in the number of resonances in both the ^1H and $^{13}C\{^1H\}$ NMR spectra of **14** compared to those of **8** indicates that **14** is less symmetric than **8**. These resonances also

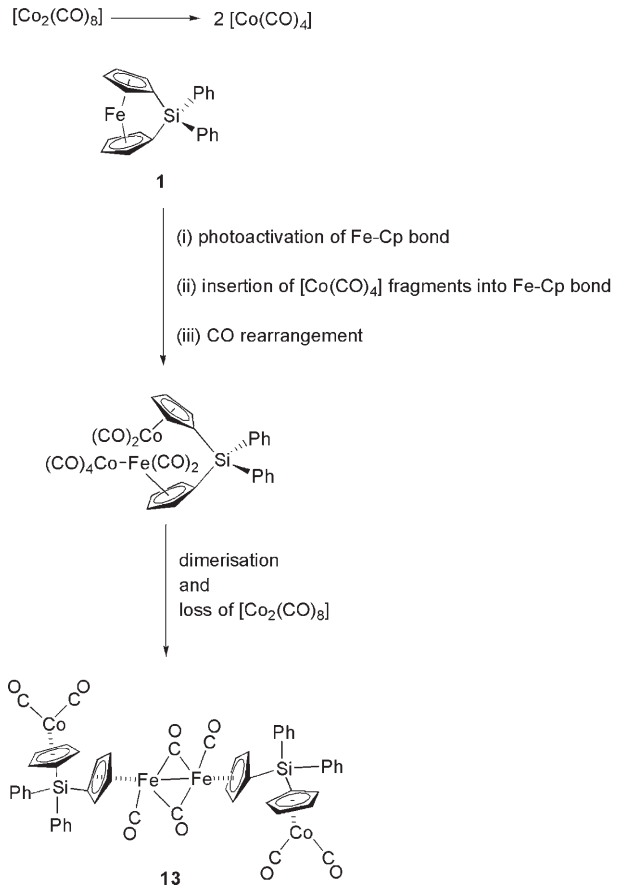

Scheme 7. Possible mechanism for the formation of **13**.

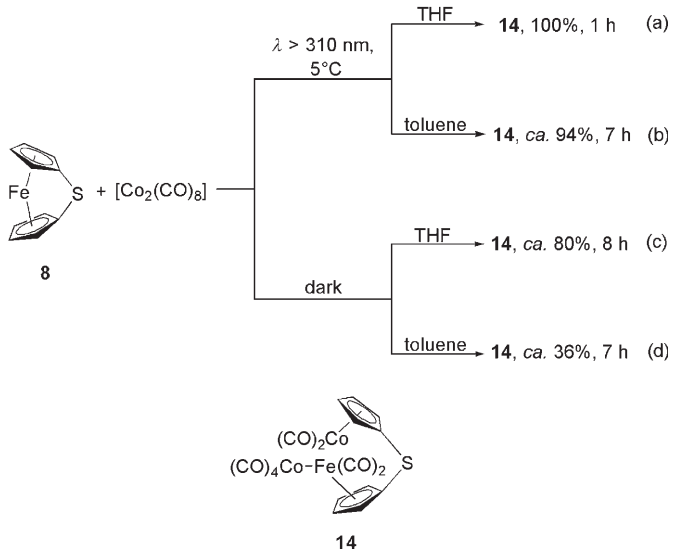

Scheme 8. Reactivity studies of **8** with $[Co_2(CO)_8]$.

indicate that there are two types of α and β Cp protons arising from inequivalent Cp rings. In addition, the general downfield shifts of Cp resonances in **14** relative to those of **8** in both the ^1H and $^{13}C\{^1H\}$ NMR spectra are typical for insertion of a metallic fragment, and was previously observed for the boron-bridged trimetallic insertion product **7**.[12] Moreover, both the IR data and the number of carbonyl resonances in the $^{13}C\{^1H\}$ NMR spectrum of **14** also closely resemble that of the boron-bridged analogue **7**. The mass spectrum of **14** showed successive loss of eight carbonyls from the molecular ion ($m/z = 558$), which is evidence that a $[Co_2(CO)_8]$ fragment has been inserted. All these data strongly support the proposed structure **14**.

For comparison with the reactivity of **1**, parallel reactions for **8** were also carried out. Similar to the situation of **1**, changes to the weaker donating solvent, toluene, significantly lower the rates of reaction both in the presence and in the absence of UV irradiation (Scheme 8a vs. b and c vs. d). In contrast to the former case of **1** in which no apparent reaction occurred in the dark, **8** and $[Co_2(CO)_8]$ formed the analogous insertion product **14** in the absence of light, albeit at a slower rate (Scheme 8a vs. c and b vs. d). This further illustrates the need for the photoactivation of **1** to allow Fe–Cp bond insertion reactions. In contrast, the more highly strained thia[1]ferrocenophane **8** undergoes Fe–Cp bond insertion reactions in the absence of light, although they occur more rapidly on photochemical irradiation.

Conclusions

A series of photochemical studies have been performed on sila[1]ferrocenophane **1** and thia[1]ferrocenophane **8**, in the presence of metal carbonyls ($[Fe(CO)_5]$, $[Fe_2(CO)_9]$ and $[Co_2(CO)_8]$) as co-reactants. Whereas most of the previously reported ring-opening reactions of [1]ferrocenophanes occur via cleavage of *ipso*-Cp-C–bridging-atom bond, we have shown in this work that both **1** and **8** can undergo insertions and cleavage reactions at the Fe–Cp bond with relief of ring strain. When irradiated with UV light, the Fe–Cp bonds of **1** and **8** are selectively weakened, allowing the insertion of metal carbonyl fragments. The selective weakening is sufficient to cause oligomerisation of the highly strained **8** in THF while the less strained **1** is resistant to this process under the same conditions. In addition, **8** underwent insertion reactions with $[Fe_2(CO)_9]$ and $[Co_2(CO)_8]$ in the absence of light, but at a considerably slower rate. Attempts to induce analogous reactions of **1** in the absence of light gave only unreacted starting material. These marked differences lead to two key conclusions. Firstly, photochemical activation of the Fe–Cp bond is observed in the case of both **1** and **8**. Secondly, whereas photoirradiation is necessary for Fe–Cp bond cleavage and insertion reactions of **1**, the highly strained species **8** possesses an inherently sufficiently weakened Fe–Cp bond for analogous reactions to occur in the absence of light, albeit more slowly. Our studies also suggest that the rate of the Fe–Cp bond insertions is faster if a stronger donor solvent is used.

Future work in this area is directed towards an investigation of the mechanism of these photolytic reactions of [1]ferrocenophanes and in particular, the nature of the photoexci-

tation process.[64] Reactivity of the type illustrated in this paper may be generally applicable to related strained metallocenophanes[2–11] and species with other π-hydrocarbon ligands[26–35] and even unstrained species. Moreover, photochemical activation of metal-Cp bonds may ultimately be important not only for molecular synthesis and ring-opening polymerisation but also for the design of new catalytic processes.

Experimental Section

General methods: $[Co_2(CO)_8]$ was purchased from Strem and sublimed immediately before use. Ph_2SiCl_2 was purchased from Aldrich and distilled prior to use. $[Fe(CO)_5]$, $[Fe_2(CO)_9]$and $Na[SO_2Ph]$ were purchased from Aldrich and used as received. SCl_2 was purchased from Aldrich and distilled prior to use. $S(SO_2Ph)_2$ was prepared according to literature procedures.[65] All manipulations were performed under an atmosphere of prepurified nitrogen by using Schlenk techniques or in an inert atmosphere glovebox. Solvents were dried using the Grubbs method[66] or standard methods followed by distillation. ^1H (300 MHz), ^{13}C (75.5 MHz) and ^{29}Si (59.6 MHz) NMR spectra were recorded on a Jeol Eclipse 300, Varian Gemini 300 or Mercury 300 spectrometer. ^1H (400 MHz), ^{13}C (100.5 MHz), and ^{29}Si (79.4 MHz) NMR spectra were recorded on a Varian Unity 400 spectrometer. The ^1H resonances were referenced internally to the residual protonated solvent resonances. The ^{13}C resonances were referenced internally to the deuterated solvent resonances. ^{29}Si resonances were referenced externally to the TMS resonance. Mass spectra were recorded either with a VG 70–250S or a Bruker–Daltonic Apex IV mass spectrometer in electron impact (EI) or electrospray ionisation (ESI) mode respectively. The calculated isotopic distribution for each ion was in agreement with experimental values. Infrared spectra were recorded using a Perkin–Elmer Spectrum One FT-IR spectrometer. The irradiation experiments were carried out through the use of a Philips high-pressure (HPK 125) Hg lamp. The samples being photolysed were positioned adjacent to the light source. Elemental analyses were performed using a Perkin-Elmer 2400 C/H/N analyser.

Synthesis of 1: Neat Ph_2SiCl_2 (8.5 g, 34 mmol) was added dropwise to an orange suspension of $[Fe(\eta\text{-}C_5H_4Li)_2]$·TMEDA (10 g, 32 mmol) in diethyl ether (250 mL) at −78 °C. The yellowish orange slurry was then allowed to warm up slowly. Drastic colour change occurred between −15 to −10 °C during which the slurry becomes orange red. After warming to 22 °C, the resulting mixture was stirred for 2 h. This was subsequently filtered through a glass frit with the aid of celite to remove LiCl, giving a clear dark orange solution. The filtrate was then pumped to dryness leaving a red brown solid, which was then purified by sublimation at 120 °C under static vacuum, yielding air stable dark orange needles of **1** (3.0 g, 26 %). ^1H NMR (300 MHz, C_6D_6, 20 °C): $\delta = 4.10$ (t, 4H; Cp), 4.40 (t, 4H; Cp), 7.26 (m, 6H; Ph), 8.05 ppm (m, 4H; Ph). close to that reported in the literature.[63]

Improved synthesis of 8: A solution of $S(SO_2Ph)_2$ (2.45 g, 7.80 mmol) in THF (15 mL) was added dropwise to an orange suspension of $[Fe(\eta\text{-}C_5H_4Li)_2]$·TMEDA (2.01 g, 6.40 mmol) in THF/hexane (60 mL : 40 mL) at −78 °C. The reaction mixture turned deep red immediately. The resulting solution was stirred for 3 h at −78 °C after which hexane (2×10 mL, −78 °C) was slowly added. The deep red solution was then stirred for another 10 minutes. The precipitate of $Li[SO_2Ph]$ was allowed to settle, and the deep purple supernatant solution was filtered through a precooled (−78 °C) glass frit containing a two-inch pad of neutral alumina. The residue from the reaction flask was washed several times with precooled hexane (≈2×10 mL) and the solution was filtered. The resulting deep purple filtrate was pumped to dryness at −15 °C affording a deep purple solid. This was taken up in hexane (≈50 mL) and the resulting solution filtered through glass wool to give a deep purple solution which was then passed through an alumina column (≈4 cm). After that the deep purple eluent was pumped to dryness yielding analytically pure **8** (400 mg, 30 % yield). Attempted preparations of **8** in pure toluene (250 mL) and toluene/hexane (150 mL: 100 mL) failed to give **8**. ^1H NMR (300 MHz, C_6D_6, 20 °C): $\delta = 3.96$ (t, 4H; Cp), 4.61 ppm (t, 4H; Cp).[61]

Photochemical reaction of 1 with $[Fe(CO)_5]$ in THF: Compound **1** (35 mg, 0.096 mmol) was dissolved in THF (4 mL). The resulting orange solution was then transferred to a Schlenk tube. In the absence of light, neat $[Fe(CO)_5]$ (3 g, 15 mmol) was added dropwise to the solution of **1**, which was then photolysed at 5 °C for 5 h. After that, the dark brown reaction mixture was pumped to dryness. A ^1H NMR spectrum of this crude product revealed predominant peaks that indicated the formation of **9**. The crude product was then taken up in toluene/hexane (1.5:1.5 mL), filtered through glasswool to remove a small amount of insoluble materials, and then recrystallised at −40 °C. Dark brown needles of **9** of 100 % purity grew within a week (33 mg, 65 % yield). ^1H NMR (300 MHz, C_6D_6, 20 °C) $\delta = 4.94$ (ps t, 4H; Cp), 5.12 (ps t, 4H; Cp), 7.42 (m, 4H; Ph), 7.48 ppm (m, 6H; Ph); $^{13}C\{^1H\}$ NMR (75 MHz, C_6D_6, 20 °C) $\delta = 100.3$ (Cp), 86.5 (Cp), 84.6 (*ipso*-Cp-C), 130.3 (Ph), 136 (Ph), 132 ppm (Ph); $^{29}Si\{^1H\}$ NMR (59.6 MHz, $CDCl_3$, 21 °C) $\delta = -18.7$ ppm; IR (toluene, 20 °C): $\tilde{\nu} = 1942$, 1857 (CO), 1802, 1735 cm^{-1} (μ-CO) ; MS (70 eV, EI): *m*/*z*(%): 534 (26) $[M^+]$, 506 (8) $[M^+-CO]$, 478 (60) $[M^+-2\ CO]$, 450 (27) $[M^+-3\ CO]$, 422 (100) $[M^+-4\ CO]$; HRMS calcd for $C_{26}H_{18}O_4{}^{56}Fe_2Si_2$: 533.9669; found: 533.9659; elemental analysis calcd (%) for $C_{26}H_{18}O_4Fe_2Si_2$: C 58.5, H 3.4; found: C 58.5, H 3.5.

It should be noted that treatment of **1** in the presence of UV light in THF at 5 °C for 5 h and the reaction of **1** with $[Fe_2(CO)_9]$ in THF for 12 h in the absence of light both yielded only unreacted **1** by ^1H NMR spectroscopy.

Photochemical reaction of 8 with $[Fe(CO)_5]$ in THF: In the dark, $[Fe(CO)_5]$ (33 mg, 0.17 mmol) and **8** (30 mg, 0.14 mmol) were dissolved in THF (3 mL) in a Schlenk tube. The purple solution was irradiated with UV light at 5 °C for 5 h. The solvent was removed under high vacuum to leave green brown solid which was a mixture of **10** and **11** (≈70:30) as determined by ^1H NMR spectroscopy. The crude mixture was first dissolved in hexane (3 mL) giving a light brown supernatant, which was then decanted. Slow solvent evaporation of the light brown solution at 22 °C yielded light brown crystals of **11** suitable for single-crystal X-ray diffraction studies. The residue from the hexane extraction was then taken up in toluene (3 mL) and subsequently filtered through glasswool to remove a small amount of insoluble material giving an orange solution. Recrystallisation of this orange filtrate at −40 °C yielded single-crystals of the cyclic dimer **10** for X-ray diffraction studies (11 mg, 38 % yield).

*Data for complex **10***: ^1H NMR (300 MHz, C_6D_6, 20 °C): $\delta = 3.90$ (t, 8H; Cp), 4.56 ppm (t, 8H; Cp); $^{13}C\{^1H\}$ NMR (75 MHz, C_6D_6, 20 °C): $\delta = 68.0$ (Cp), 68.8 (Cp), 87.3 ppm (*ipso*-Cp-C); MS (70 eV, EI): *m*/*z* (%): 432 (91) $[M^+]$, 336 (100) $[M^+-Cp]$; elemental analysis calcd (%) for $C_{20}H_{16}Fe_2S_2$: C 55.6, H 3.7; found: C 55.9, H 4.1.

*Data for complex **11***: ^1H NMR (300 MHz, C_6D_6, 20 °C): $\delta = 4.43$ (br t, 4H; Cp), 4.73 ppm (br t, 4H; Cp); $^{13}C\{^1H\}$ NMR (75 MHz, C_6D_6, 20 °C): $\delta = 99.7$ (Cp), 83.5 (Cp), 96.1 ppm (*ipso*-Cp-C), not observed (CO); IR (hexane, 25 °C): $\tilde{\nu} = 1978$ (CO), 1806 cm^{-1} (μ-CO); MS (70 eV, EI): *m*/*z*(%): 384 (12) $[M^+]$, 356 (13) $[M^+-CO]$, 328 (29) $[M^+-2\ CO]$, 272 (100) $[M^+-4\ CO]$; HRMS calcd for $C_{14}H_8{}^{56}Fe_2SO_4$: 383.8842; found: 383.8846.

Photolytic reaction of 8 in THF: In the absence of light, **8** (52 mg, 0.24 mmol) was dissolved in THF (10 mL) to yield a red purple solution. After irradiation with UV light at 5 °C for 3 h, the solution of **8** turned into a green brown suspension. This was then pumped to dryness and then taken up in toluene (8 mL) to give an orange supernatant with green brown precipitate. The former was carefully decanted and then pumped to dryness, giving an orange powder, which was shown by ^1H NMR spectroscopy to be **10** (28 mg, 54 %). The green brown precipitate (19 mg) was also dried in vacuo and was found to be insoluble in common organic solvents. This green brown material was analysed by pyrolysis MS and was found to contain mainly ring-opened oligomers derived from **8**. A control reaction (monitored by ^1H NMR spectroscopy) in the absence of light was also performed and only starting materials were recovered after 12 h.

Data for the oligomers of ***8*****:** Pyrolysis MS (70 eV, EI, 400 °C): *m*/*z* (%): 648 (30) [*n* = 3], 432 (100) [*n* = 2].

Photochemical reaction of 8 in toluene: In the absence of light, **8** was dissolved in [D_8]toluene and the resulting purple solution was transferred to an NMR tube equipped with a Youngs tap. This was then kept in the dark. A ^{1}H NMR spectrum after 12 h showed only unreacted **8**. This was then irradiated at 5 °C. After 3 h, the ^{1}H NMR spectrum showed the presence of **8**, **11** and oligomers of **8** in a ratio of ≈50:3:8 (82:5:13 %) by integration of the Cp protons.

Photochemical reaction of 8 with [$Fe_2(CO)_9$]: In the absence of light, a solution of **8** (20 mg, 0.093 mmol) in THF was added to a suspension of [$Fe_2(CO)_9$] (67 mg, 0.185 mmol) in THF. The resultant red orange slurry was photolysed for 3 h at 5 °C, during which it turned dark maroon. A ^{1}H NMR spectrum of the crude mixture indicated the formation of **11** and **10** in a ratio of ≈85:15.

Analogous reaction in the absence of light showed the formation of **11** and unreacted **8** in a ratio of ≈30:70.

Photochemical reaction of 8 with [$Fe(CO)_5$] in toluene: In the dark, [$Fe(CO)_5$] (31 mg, 0.158 mmol) and **8** (12 mg, 0.056 mmol) were dissolved in toluene (2 mL) in a Schlenk tube. The resultant purple solution was irradiated with UV light at 5 °C for 5 h. A maroon paste was produced after the removal of volatile materials under high vacuum. This crude product was analysed by ^{1}H NMR spectroscopy to be a mixture of **11** (≈77 %) and other unidentified byproducts (≈23 % estimated by total integration of ^{1}H NMR protons versus those for **11**).

Photochemical reaction of 1 with [$Co_2(CO)_8$]: In the dark, [$Co_2(CO)_8$] (30 mg, 0.088 mmol) and **1** (30 mg, 0.082 mmol) were dissolved in THF (5 mL) in a Schlenk tube. The resulting black solution was then irradiated with UV light at 5 °C for 7 h and then all volatile materials were removed in *vacuo*. A ^{1}H NMR spectrum of this crude product showed the presence of **13** in 80 % spectroscopic yield. The residue was then dissolved in hexane (1 mL) and filtered through glasswool to remove small quantities of insoluble impurities. Recrystallisation from the filtrate yielded dark brown crystals of **13** (16 mg, 36 % yield) suitable for single-crystal X-ray diffraction.

An analogous reaction in [D_8]toluene was also performed. After 7 h, only 7 % conversion to **13** was observed by ^{1}H NMR spectroscopy.

It is noteworthy that in the absence of light, no apparent reaction occurred (from ^{1}H NMR spectroscopy) after stirring **1** with [$Co_2(CO)_8$] for 8 h in either THF or toluene.

Data for complex ***13***: ^{1}H NMR (300 MHz, C_6D_6, 20 °C): δ = 4.73 (ps t, 8H; Cp), 4.50 (dt, 8H; Cp), 7.68 (m, 8H; Ph), 7.20 ppm (m, 12H; Ph); ^{13}C{^{1}H} NMR (75 MHz, C_6D_6, 20 °C): δ = 92.8 (Cp), 91.9 (Cp), 90.6 (Cp), 89.8 (Cp), 84.4 (*ipso*-Cp-C), 87.4 (*ipso*-Cp-C), 128.4 (Ph), 130.9 (Ph), 132.5 (*ipso*-Ph-C), 136.1 (Ph), 204.2 (Co–CO), 212.2 ppm (Fe–CO). ^{29}Si{^{1}H} NMR (79.4 MHz, C_6D_6, 20 °C): δ = −20.6 ppm; IR (toluene, 25 °C): $\tilde{\nu}$ = 2070, 2064, 2055, 2032, 2017 (*t*-CO), 1975, 1867, 1830 cm^{-1} (μ-CO); MS data were not obtainable because **13** decomposed in the spectrometer; elemental analysis was not possible as repeated experiments consistently gave **13** of ≈95 % purity.

Photochemical reaction of 8 with [$Co_2(CO)_8$]: [$Co_2(CO)_8$] (16 mg, 0.047 mmol) and **8** (10 mg, 0.046 mmol) were dissolved in THF (≈0.5 mL) and C_6D_6 (≈0.1 mL) in a sealable NMR tube in the absence of light. The resulting red brown solution was irradiated with UV light at 5 °C for 1 h. Analysis by ^{1}H NMR spectroscopy showed the formation of **14** in 100 % conversion. The volatile materials were then removed under high vacuum leaving a red brown paste of **14** (15 mg, 58 % yield).

Analogous reaction in [D_8]toluene gave **14** in 94 % spectroscopic yield after 7 h.

In the absence of light, parallel NMR scale reactions in THF and [D_8]toluene gave **14** in 80 % and 36 % conversion respectively after 7 h.

Data for complex ***14***: ^{1}H NMR (300 MHz, C_6D_6, 20 °C): δ = 3.99 (br t, 2H; Cp), 4.11 (br t, 2H; Cp), 4.34 (br t, 2H; Cp), 4.62 ppm (br t, 2H; Cp); ^{13}C{^{1}H} NMR (75 MHz, C_6D_6, 20 °C): δ = 84.7 (Cp), 86.2 (Cp), 86.3 (Cp), 89.1 (Cp), 92.8, 105.9 (*ipso*-Cp-C), 203.4 (Co–CO), 212.9 ppm (Fe–CO); IR (hexane, 25 °C): $\tilde{\nu}$ = 2067, 2034, 2011, 1977, 1936, 1870, 1849, 1824, 1795, 1729 cm^{-1} (CO); MS (70 eV, EI): *m*/*z* (%): 530 (1) [M^+ −CO], 502 (3) [M^+−2 CO], 474 (7) [M^+−3 CO], 446 (8) [M^+−4 CO], 418 (6) [M^+−5 CO], 390 (8) [M^+−6 CO], 362 (10) [M^+−7 CO], 334 (40) [M^+−8 CO], 275 (100) [M^+−8 CO−Co]; HRMS (4.6 kV, ESI): calcd for

Table 3. Data Collection & Refinement Parameters for **10**, **11** and **13**.

	10	**11**	**13**
formula	$C_{20}H_{16}Fe_2S_2$	$C_{14}H_8Fe_2O_4S{\cdot}C_6H_{14}$	$C_{52}H_{36}Co_2Fe_2O_8Si_2$
M_r	432.15	470.14	1074.55
T [K]	173(2)	150(2)	150(2)
crystal system	orthorhombic	monoclinic	triclinic
space group	*Pnma*	*C*2/*m*	$P\bar{1}$
a [Å]	10.574(2)	17.4003(10)	9.3269(19)
b [Å]	20.146(4)	12.0168(5)	10.696(2)
c [Å]	7.4714(15)	7.8706(4)	13.278(2)
α [°]	90	90	67.041(9)
β [°]	90	96.895(3)	70.165(8)
γ [°]	90	90	71.332(9)
V [Å^3]	1591.6(5)	1633.81(14)	1120.1(4)
Z	4	4	1
ρ_{calcd} [g cm^{-3}]	1.803	1.911	1.593
$\mu(Mo_{K\alpha})$ [mm^{-1}]	2.082	1.931	1.473
F(000)	880	968	546
crystal size [mm^3]	0.30×0.30×0.01	0.16×0.14×0.10	0.12×0.12×0.01
θ range [°]	2.02 to 27.48	2.61 to 27.53	2.57 to 25.20
reflections collected	15426	6469	11373
independent reflections (R_{int})	1863 (0.0635)	1946 (0.0504)	3941 (0.1234)
absorption correction	semi-empirical from equivalents	semi-empirical from equivalents	semi-empirical from equivalents
max/min transmission	0.980/0.584	0.834/0.626	1.013/0.632
parameters refined	112	115	299
GoF on F^2	1.496	1.040	0.944
$R1$[a] [$I > 2\sigma(I)$]	0.0438	0.0388	0.0540
$wR2$[b] (all data)	0.0971	0.1059	0.1330
peak and hole [e Å^{-3}]	0.743 and −0.593	0.457 and −0.508	0.462 and −0.478

[a] $R1 = \Sigma\,||F_o| - |F_c||/\Sigma|F_o|$; [b] $wR2 = \{\Sigma[w(F_o^2 - Fc^2)^2]/\Sigma[w(F_o^2)^2]\}^{1/2}$.

$C_{18}H_7{}^{56}FeCo_2SO_8$: 556.7861760; found: 556.7880540; elemental analysis was not possible as repeated experiments consistently gave 95% pure **14**.

X-ray crystallography: Selected crystal, data collection, and refinement parameters for **10**, **11** and **13** are given in Table 3. Single-crystal X-ray diffraction data were collected using a Nonius Kappa-CCD diffractometer and monochromated $Mo_{K\alpha}$ radiation ($\lambda = 0.71073$). The data were integrated and scaled using the Denzo-SMN package.[67] The SHELXTL/PC package was used to solve and refine the structures.[68] Refinement was by full-matrix least-squares on F^2 using all data (negative intensities included). Hydrogen atoms were placed in calculated positions and included in the refinement in riding motion approximations.

During the refinement of **11**, an area of electron density was located in difference Fourier maps that was assigned as a solvent molecule. The peak pattern of electron density suggested that the solvent molecule was highly disordered; attempts to model the disorder were unsuccessful. In the final cycles of refinement, the contribution to electron density corresponding to a disordered hexane molecule was removed from the observed data using the SQUEEZE option in PLATON.[69] The resulting data vastly improved the precision of the geometric parameters of the remaining structure. The contribution of a hexane molecule has been included in the molecular formula. Data for the crystal structures described is shown in Table 3.

CCDC 655522, 655524, 655525 contain the supplementary crystallographic data for this paper. These data can be obtained free of charge from The Cambridge Crystallographic Data Centre via www.ccdc.cam.ac.uk/data_request/cif.

Acknowledgement

I.M. thanks the EU for a Marie Curie Chair and the Royal Society for a Wolfson Research Merit Award and the University of Bristol for start up funds.

[1] A. G. Osborne, R. H. Whiteley, *J. Organomet. Chem.* **1975**, *101*, C27–C28.
[2] S. L. J. Conway, T. Dijkstra, L. H. Doerrer, J. C. Green, M. L. H. Green, A. H. H. Stephens, *J. Chem. Soc. Dalton Trans.* **1998**, 2689–2696.
[3] S. L. J. Conway, L. H. Doerrer, J. C. Green, M. L. H. Green, A. Scottow, A. H. H. Stephens, *J. Chem. Soc. Dalton Trans.* **2000**, 329–333.
[4] M. J. Drewitt, S. Barlow, D. O'Hare, J. M. Nelson, P. Nguyen, I. Manners, *Chem. Commun.* **1996**, 2153–2154.
[5] S. Fox, J. P. Dunne, M. Tacke, D. Schmitz, R. Dronskowski, *Eur. J. Inorg. Chem.* **2002**, 3039–3046.
[6] D. M. Heinekey, C. E. Radzewich, *Organometallics* **1999**, *18*, 3070–3074.
[7] S. C. Jones, S. Barlow, D. O'Hare, *Chem. Eur. J.* **2005**, *11*, 4473–4481.
[8] K. M. Kane, P. J. Shapiro, A. Vij, R. Cubbon, A. L. Rheingold, *Organometallics* **1997**, *16*, 4567–4571.
[9] J. M. Nelson, A. J. Lough, I. Manners, *Angew. Chem.* **1994**, *106*, 1019–1021; *Angew. Chem. Int. Ed.* **1994**, *33*, 989–991.
[10] P.-J. Sinnema, P. J. Shapiro, D. M. J. Foo, B. Twamley, *J. Am. Chem. Soc.* **2002**, *124*, 10996–10997.
[11] U. Vogel, A. J. Lough, I. Manners, *Angew. Chem.* **2004**, *116*, 3383–3387; *Angew. Chem. Int. Ed.* **2004**, *43*, 3321–3325.
[12] A. Berenbaum, H. Braunschweig, R. Dirk, U. Englert, J. C. Green, F. Jäkle, A. J. Lough, I. Manners, *J. Am. Chem. Soc.* **2000**, *122*, 5765–5774.
[13] R. Broussier, A. Da Rold, B. Gautheron, Y. Dromzee, Y. Jeannin, *Inorg. Chem.* **1990**, *29*, 1817–1822.
[14] A. Bucaille, T. Le Borgne, M. Ephritikhine, J. C. Daran, *Organometallics* **2000**, *19*, 4912–4914.
[15] I. R. Butler, W. R. Cullen, F. W. B. Einstein, S. J. Rettig, A. J. Willis, *Organometallics* **1983**, *2*, 128–135.
[16] W. Finckh, B.-Z. Tang, D. A. Foucher, D. B. Zamble, R. Ziembinski, A. J. Lough, I. Manners, *Organometallics* **1993**, *12*, 823–829.
[17] A. B. Fischer, J. B. Kinney, R. H. Staley, M. S. Wrighton, *J. Am. Chem. Soc.* **1979**, *101*, 6501–6506.
[18] D. A. Foucher, M. Edwards, R. A. Burrow, A. J. Lough, I. Manners, *Organometallics* **1994**, *13*, 4959–4966.
[19] F. Jäkle, R. Rulkens, G. Zech, D. A. Foucher, A. J. Lough, I. Manners, *Chem. Eur. J.* **1998**, *4*, 2117–2128.
[20] R. Rulkens, D. P. Gates, D. Balaishis, J. K. Pudelski, D. F. McIntosh, A. J. Lough, I. Manners, *J. Am. Chem. Soc.* **1997**, *119*, 10976–10986.
[21] I. Sänger, J. B. Heilmann, M. Bolte, H.-W. Lerner, M. Wagner, *Chem. Commun.* **2006**, 2027–2029.
[22] J. A. Schachner, C. L. Lund, J. W. Quail, J. Müller, *Organometallics* **2005**, *24*, 785–787.
[23] J. A. Schachner, C. L. Lund, J. W. Quail, J. Müller, *Organometallics* **2005**, *24*, 4483–4488.
[24] D. Seyferth, H. P. Withers, Jr., *J. Organomet. Chem.* **1980**, *185*, C1-C5.
[25] H. K. Sharma, F. Cervantes-Lee, J. S. Mahmoud, K. H. Pannell, *Organometallics* **1999**, *18*, 399–403.
[26] A. Bartole-Scott, H. Braunschweig, T. Kupfer, M. Lutz, I. Manners, T.-l. Nguyen, K. Radacki, F. Seeler, *Chem. Eur. J.* **2006**, *12*, 1266–1273.
[27] A. Berenbaum, I. Manners, *Dalton Trans.* **2004**, 2057–2058.
[28] H. Braunschweig, M. Homberger, C. Hu, X. Zheng, E. Gullo, G. Clentsmith, M. Lutz, *Organometallics* **2004**, *23*, 1968–1970.
[29] H. Braunschweig, T. Kupfer, M. Lutz, R. Krysztov, S. Fabian, S. Rainer, *Angew. Chem.* **2006**, *118*, 8217–8220; *Angew. Chem. Int. Ed.* **2006**, *45*, 8048–8051.
[30] C. Elschenbroich, F. Paganelli, M. Nowotny, B. Neumüller, O. Burghaus, *Z. Anorg. Allg. Chem.* **2004**, *630*, 1599–1606.
[31] C. Elschenbroich, E. Schmidt, R. Gondrum, B. Metz, O. Burghaus, W. Massa, S. Wocadlo, *Organometallics* **1997**, *16*, 4589–4596.
[32] C. L. Lund, J. A. Schachner, J. W. Quail, J. Müller, *Organometallics* **2006**, *25*, 5817–5823.
[33] M. Tamm, A. Kunst, T. Bannenberg, E. Herdtweck, P. Sirsch, C. J. Elsevier, J. M. Ernsting, *Angew. Chem.* **2004**, *116*, 5646–5650; *Angew. Chem. Int. Ed.* **2004**, *43*, 5530–5534.
[34] M. Tamm, A. Kunst, T. Bannenberg, S. Randoll, P. G. Jones, *Organometallics* **2007**, *26*, 417–424.
[35] M. Tamm, A. Kunst, E. Herdtweck, *Chem. Commun.* **2005**, 1729–1731.
[36] J. C. Green, *Chem. Soc. Rev.* **1998**, *27*, 263–272.
[37] S. Barlow, M. J. Drewitt, T. Dijkstra, J. C. Green, D. O'Hare, C. Whittingham, H. H. Wynn, D. P. Gates, I. Manners, J. M. Nelson, J. K. Pudelski, *Organometallics* **1998**, *17*, 2113–2120.
[38] M. J. MacLachlan, M. Ginsbury, J. Zheng, O. Knöll, A. J. Lough, I. Manners, *New J. Chem.* **1998**, *22*, 1409–1415.
[39] J. K. Pudelski, I. Manners, *J. Am. Chem. Soc.* **1995**, *117*, 7265–7266.
[40] D. A. Foucher, B.-Z. Tang, I. Manners, *J. Am. Chem. Soc.* **1992**, *114*, 6246–6248.
[41] R. Rulkens, Y. Ni, I. Manners, *J. Am. Chem. Soc.* **1994**, *116*, 12121–12122.
[42] P. Gómez-Elipe, P. M. Macdonald, I. Manners, *Angew. Chem.* **1997**, *109*, 780–783; *Angew. Chem. Int. Ed.* **1997**, *36*, 762–764.
[43] K. Temple, F. Jäkle, J. B. Sheridan, I. Manners, *J. Am. Chem. Soc.* **2001**, *123*, 1355–1364.
[44] J. B. Sheridan, A. J. Lough, I. Manners, *Organometallics* **1996**, *15*, 2195–2197.
[45] T. Mizuta, M. Onishi, K. Miyoshi, *Organometallics* **2000**, *19*, 5005–5009.
[46] T. Mizuta, Y. Imamura, K. Miyoshi, *J. Am. Chem. Soc.* **2003**, *125*, 2068–2069.
[47] M. Tanabe, G. W. M. Vandermeulen, W. Y. Chan, P. W. Cyr, L. Vanderark, D. A. Rider, I. Manners, *Nat. Mater.* **2006**, *5*, 467–470.
[48] M. Tanabe, I. Manners, *J. Am. Chem. Soc.* **2004**, *126*, 11434–11435.
[49] M. Tanabe, S. C. Bourke, D. E. Herbert, I. Manners, *Angew. Chem.* **2005**, *117*, 6036–6040; *Angew. Chem. Int. Ed.* **2005**, *44*, 5886–5890.

[50] A. Berenbaum, F. Jäkle, A. J. Lough, I. Manners, *Organometallics* **2002**, *21*, 2359–2361.
[51] J. Weaver, P. Woodward, *J. Chem. Soc. Dalton Trans.* **1973**, 1439–1443.
[52] J. S. McKechnie, B. H. Bersted, I. C. Paul, W. E. Watts, *J. Organomet. Chem.* **1967**, *8*, P29–P31.
[53] D. L. Zechel, D. A. Foucher, J. K. Pudelski, G. P. A. Yap, A. L. Rheingold, I. Manners, *J. Chem. Soc. Dalton Trans.* **1995**, 1893–1899.
[54] M. Scheibitz, R. F. Winter, M. Bolte, H.-W. Lerner, M. Wagner, *Angew. Chem.* **2003**, *115*, 954–957; *Angew. Chem. Int. Ed.* **2003**, *42*, 924–927.
[55] J. A. Schachner, G. A. Orlowski, J. W. Quail, H.-B. Kraatz, J. Müller, *Inorg. Chem.* **2006**, *45*, 454–459.
[56] J.-M. Löwendahl, M. Håkasson, *Organometallics* **1995**, *14*, 4736–4741.
[57] J. Park, Y. Seo, S. Cho, D. Whang, K. Kim, T. Chang, *J. Organomet. Chem.* **1995**, *489*, 23–25.
[58] T. Mizuta, Y. Imamura, K. Miyoshi, H. Yorimitsu, K. Oshima, *Organometallics* **2005**, *24*, 990–996.
[59] H. Brunner, J. Klankermayer, M. Zabel, *J. Organomet. Chem.* **2000**, *601*, 211–219.
[60] U. T. Mueller-Westerhoff, *Angew. Chem.* **1986**, *98*, 700–716; *Angew. Chem. Int. Ed.* **1986**, *25*, 702–717.
[61] J. K. Pudelski, D. P. Gates, R. Rulkens, A. J. Lough, I. Manners, *Angew. Chem.* **1995**, *107*, 1633–1635; *Angew. Chem. Int. Ed.* **1995**, *34*, 1506–1508.
[62] R. F. Bryan, P. T. Greene, D. S. Field, M. J. Newlands, *J. Chem. Soc. D. Chem. Commun.* **1969**, 1477.
[63] D. A. Foucher, R. Ziembinski, B.-Z. Tang, P. M. Macdonald, J. Massey, C. R. Jaeger, G. J. Vancso, I. Manners, *Macromolecules* **1993**, *26*, 2878–2884.
[64] Y. Yamaguchi, W. Ding, C. T. Sanderson, M. L. Borden, M. J. Morgan, C. Kutal, *Coord. Chem. Rev.* **2007**, *251*, 515–524.
[65] S. Inaoka, D. M. Collard, *J. Mater. Chem.* **1999**, *9*, 1719–1726.
[66] A. B. Pangborn, M. A. Giardello, R. H. Grubbs, R. K. Rosen, F. J. Timmers, *Organometallics* **1996**, *15*, 1518–1520.
[67] Z. Otwinowski, W. Minor, *Methods Enzymol.* **1997**, *276*, 307–326.
[68] G. M. Sheldrick, *SHELXTL/PC* V 5.1, Bruker Analytical X-ray Systems, Madison, **1997**.
[69] A. L. Spek, *J. Appl. Crystallogr.* **2003**, *36*, 7–13.

Received: June 22, 2007
Published online: November 14, 2007

